

論文の内容の要旨

Optical Control of Neurite Outgrowth Direction in Living Organisms with Light-Induced Protein Oligomerization System

(タンパク質光多量体形成反応を用いた

生体内における神経軸索伸長方向の制御の確立)

氏名 遠藤 瑞己

Introduction

Precise assembly of functional neural circuits requires sequential wiring of individual axons during nervous system development. Disruption of the axon pathfinding by neurodegenerative disorders engenders severe impairments in both motor and cognitive function. Although most signaling mechanisms in axon guidance have been clarified using an *in vitro* approach, it is still difficult to investigate how it is modulated in complicated extracellular environment of living animals due to the lack of tools. To assess the dynamic influence of the surrounding complex milieu on the developing axons during their pathfinding *in vivo*, a novel method is necessary for the direct manipulation of the axon guidance signaling in living animals. Herein, in the present thesis, I developed an optical method, which enables light-induced attraction of neurites with photo-activation of an axon guidance receptor both in *in vitro* and *in vivo*.

Principle

Deleted in Colorectal Cancer (DCC) is an axon guidance receptor protein embedded in the plasma membrane. DCC oligomerizes upon its extracellular ligand binding, which is crucial for the induction of cytoskeletal remodeling, resulting in axon turning. To control the oligomerization by external light, a photoreceptor protein Cryptochrome 2 (CRY2) was used. CRY2 forms a cluster upon blue light (440–488 nm) illumination. CRY2 was connected genetically with DCC, named photoactivatable DCC (PA-DCC) (Fig. 1A). Due to the blue-light-dependent CRY2 oligomerization, the connected DCCs are activated, resulting in axonal elongation (Fig. 1B).

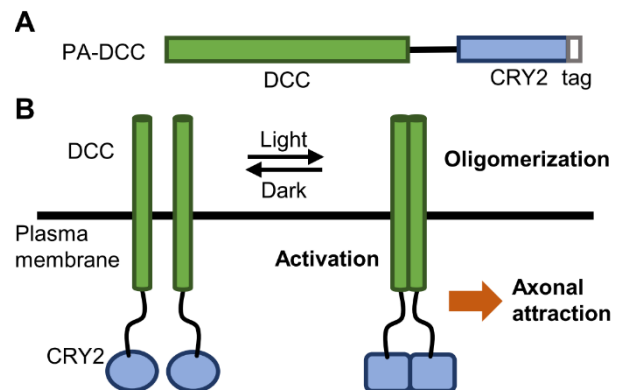


Fig. 1. Design of a system to control outgrowth with light.
A. Domain structures of PA-DCC. White squares show epitope V5 or myc tags. B. Schematic diagram for the strategy of DCC activation with blue light illumination.

Results

1. Light-dependent activation of PA-DCC molecules

To investigate the oligomerization of PA-DCC upon light stimulation, myc or V5 epitope tag was attached to the PA-DCC for co-immunoprecipitation (co-IP). DCC connected with photo-insensitive CRY2 mutant (D387A), represented as PA-DCC (D387A), and DCC without CRY2 named “DCC” were also prepared as a non-light reactive control. Cells co-expressing the tagged molecules were exposed to blue LED light (5 s min^{-1}) for 15 min before the co-IP assays. Only myc-tagged PA-DCC molecules were pulled down with V5-tagged molecules upon the blue light illumination (**Fig. 2A**). The light-induced oligomerization efficiency of PA-DCC increased along with the illumination time and with light intensity (**Fig. 2B**). In the case of DCC only or DCC connected with CRY2 (D387A), oligomerization was not observed. These results indicate that photo-conversion of CRY2 triggered PA-DCC oligomerization.

Ligand-induced DCC oligomerization triggers the phosphorylation of FAK, initiating the downstream signaling cascade for axon turning. To investigate whether light-dependent oligomerization of PA-DCC trigger the downstream signaling, phosphorylation level of FAK was examined. Results confirmed that FAK in PA-DCC expressing cells were phosphorylated with blue light illumination (**Fig. 3A**). Additionally, the phosphorylation levels of FAK elevated with increasing the number of light pulses (**Fig. 3B**). These results demonstrate that light-induced CRY2 oligomerization can trigger the DCC activation.

To confirm the reversibility of light-dependent oligomerization and activation of PA-DCC, the dissociation and the deactivation profiles after light illumination of PA-DCC were investigated. Co-IP showed time dependent dissociation of oligomerized PA-DCCs after illumination (**Fig. 4A**). Most PA-DCCs dissociated into monomer within 10 min. In addition, the phosphorylation level of FAK decreased (**Fig. 4B**). The time course of PA-DCC deactivation corresponded to that of the PA-DCC dissociation after the illumination. Taken together, blue light illumination activates PA-DCC transiently, thereby ensuring the capability of the tool to guide axons to the desired direction with repetitive illumination on growth cones.

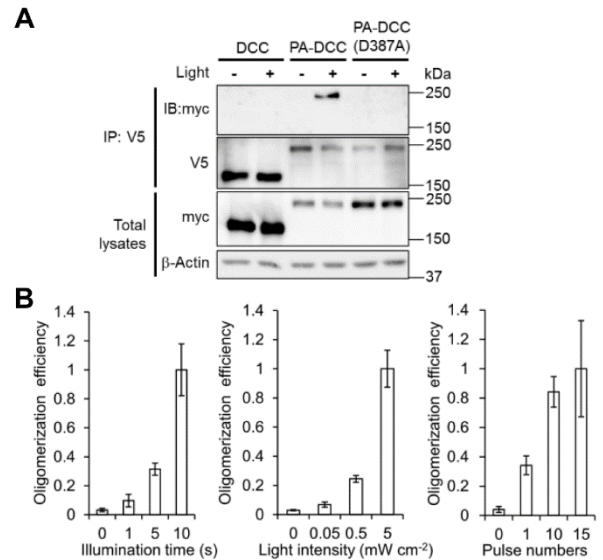


Fig. 2. Confirmation of light-induced DCC oligomerization.

A. Results of co-immunoprecipitation. V5-tagged molecules were immunoprecipitated from the lysates with the anti-V5 antibody (IP: V5). Co-immunoprecipitated myc-tagged molecules were detected by anti-myc antibody (IB: myc). **B.** Dependence of PA-DCC oligomerization efficiency on the illumination time, intensity, and pulse numbers. The efficiency was calculated for each illumination time and indicated as scores relative to the maximal value. Error bars, s.d. (n = 3).

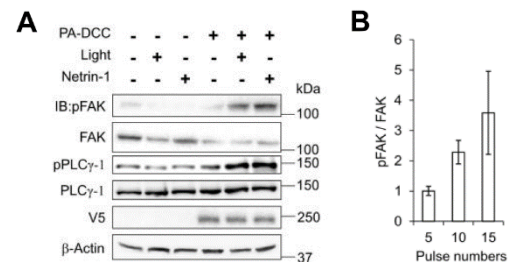


Fig. 3. Activation of PA-DCC with blue light.

A. Analysis of the phosphorylation of FAK and PLC γ -1. Cells were stimulated with light or with netrin-1 (200 ng mL^{-1}) for 15 min. Each protein or phosphorylation was detected by the specific antibody. **B.** Pulse number dependency of the FAK phosphorylation.

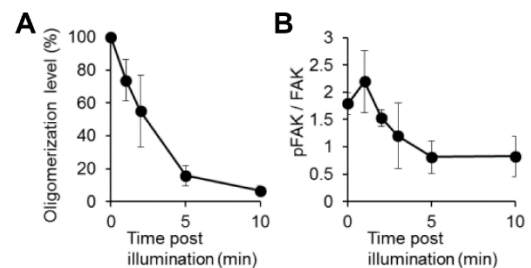


Fig. 4. Reversibility of the PA-DCC system.

A. Dissociation profile of PA-DCC oligomer. The oligomerization level was indicated relative to the level just after the illumination. Error bars, s.d. (n = 3). **B.** Dephosphorylation of FAK after light illumination. The phosphorylation level was indicated relative to the basal level. Error bars, s.d. (n = 3).

2. Axonal attraction by light-induced PA-DCC activation

To explore the possibility of the axonal attraction with PA-DCC, growth cone turning assays were performed in neurons from chick embryos (E9). cDNAs encoding PA-DCC were transfected to DRG neurons. A part of transfected growth cones was illuminated with blue light (metal halide lamp with 425–440 nm filter) in a pulse-like manner (5 s every 5 min) during the observation. Axons expressing PA-DCC turned toward the illuminated side. (**Fig. 5A**). In contrast, the blue light illumination did not affect the axonal growth direction without PA-DCC expression or with light-insensitive PA-DCC (D387A). Time lapse imaging of the light-induced axonal attraction revealed the direction of growth cone movements was dependent on each pulsatile illumination (**Fig. 5B**). To statistically analyze the effect of illumination, turning angles of the illuminated growth cones were calculated (**Fig. 5C**). The mean turning angle of growth cones with PA-DCC expression was $37.4 \pm 3.8^\circ$, which was significantly different from that of growth cones without PA-DCC expression ($-0.6 \pm 3.3^\circ$) (**Fig. 5D**). These results show that PA-DCC enabled to control the neurite outgrowth direction with light illumination in cultured neurons.

After the light-induced attraction, the illumination area was repositioned from the left side to the right side. Also, the pulse-like illuminations continued further (**Fig. 5E**). Subsequent illumination revealed that all examined growth cones, which were attracted by the first illumination at the angles of $-26.2 \pm 4.4^\circ$, turned to the repositioned illuminated side at the angles of $39.2 \pm 7.0^\circ$. The results demonstrate the capability of redirecting the growth cone with repeated light-induced turning (**Fig. 5F**). The results demonstrate the capability of redirecting the growth cone with repeated light-induced turning.

To confirm that the illumination on a part of the growth cone triggered attractive signaling locally, phosphorylation of FAK within illuminated growth cones were examined by immunocytochemistry. Compared to the growth cone without PA-DCC, FAK phosphorylation signals increased in the illuminated side, including in filopodia (**Fig. 5G**). Taken together, results show that PA-DCC can control the neurite outgrowth direction with light illumination in chick DRG neurons.

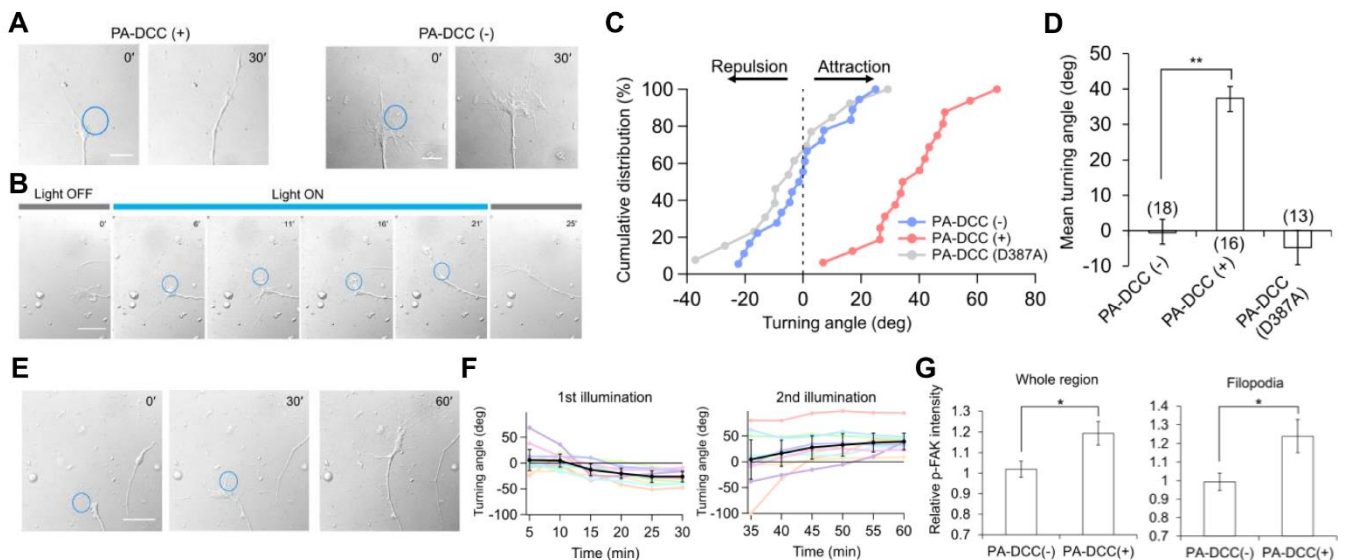


Fig. 5. Light-induced growth cone turning of chick DRG neurons expressing PA-DCC.

A. DIC images of growth cones with or without PA-DCC expression. Black circles represent illuminated regions (5 s every 5 min pulses). The images were taken at initial time (0') and 30 min after (30'). Scale bar, 5 μ m. **B.** Time lapse images of light-induced growth cone attraction with PA-DCC. Digits show elapsed minutes. The illuminations were performed at t = 6, 11, 16, 21 min. Scale bar, 10 μ m. **C.** Cumulative distribution of final growth cone turning angles in the light-induced growth cone attraction assay. Turning angles were calculated by plotting growth cone centers. **D.** Turning angles of growth cones with illumination. Numbers in parentheses indicated the total number of growth cones tested. Error bars, s.e.m. ****** $P < 0.01$, Dunnett's test. **E.** A representative data of the repeatedly illuminated growth cones. Scale bar, 10 μ m. **F.** Time course turning angle analysis of growth cones with repositioned illuminations. Each data is shown by a colored line. Averaged data are shown as black. The turning angles with positive values represents growth cones turning to the right side. Error bars, 98% confidential intervals of the mean ($n = 10$). **G.** Analysis of FAK phosphorylation level in the illuminated side. Phosphorylation intensity in the illuminated side was indicated as scores relative to the intensity in the non-illuminated side. Analyzed areas were determined by mCherry fluorescence. Error bars, s.e.m ($n = 5$). ***** $P < 0.05$, unpaired t-test.

3. In vivo photo-manipulation of the growth cone behavior.

Next, we investigated whether it is possible to control the direction of axon extension with light in living nematode worm *Caenorhabditis elegans* (*C. elegans*). For the following experiments, DCC in PA-DCC was replaced with UNC-40, a homolog of DCC in *C. elegans* and the endogenous guidance molecules were eliminated. Subsequently, a transgenic line conveying PA-UNC-40 in VD neurons was established.

Growth cones of VD neurons in anesthetized transgenic mutant worms were visualized using a co-expressed fluorescent protein, mCherry. A part of the growth cones was illuminated with blue laser light under the confocal microscope in a pulse-like manner (2 s min^{-1}). Time lapse imaging with light stimulation showed growth cones were attracted to the illuminated side (**Fig. 6A**). The temporal profile of growth cone centroid plots demonstrated clear light-induced attraction in growth cones expressing PA-UNC-40 (**Fig. 6B**). Taken altogether, blue laser light illumination enables attraction of the growth cone that expresses PA-UNC-40 in living worms.

4. Optical regulation of the growth cone motility in living organisms.

A heterogeneous extracellular milieu affects growth cone behaviors *in vivo*. For example, VD growth cones stall at the lateral nerve cord during the dorsal extension. Stalled growth cones spread along the nerve cord and become anvil-shaped.

To compare the motility towards the different directions, the anvil-shaped growth cone was sequentially illuminated on two different sides during the observation (**Fig. 7A**). While the dorsal side illumination did not induce any observable attractive response, the subsequent anterior illumination triggered marked growth cone intrusion into the illuminated area. These behaviors were also confirmed by centroid tracking from multiple experiments (**Fig. 7B**). Given that the extent of light-induced downstream signaling was not different in illuminations on either side, the nerve cord was able to impede the VD growth cone advancement, thereby restricting its motility. Consequently, the photo-manipulation system enabled direct analysis of the growth cone behavior within intrinsic extracellular environments.

Conclusion

PA-DCC was activated with blue-light illumination by the light-induced clustering of fused CRY2. Results showed that the local activation of PA-DCC changed the direction of the neuronal growth in both chick and *C. elegans*. This is the first report of the method that achieves optical manipulation of growth cone behavior *in vivo*. Further optimization of the photo-manipulation system will enable the optical wiring of the neurons in living animals, which contributes to the development of regenerative therapies for neurodegenerative disorders.

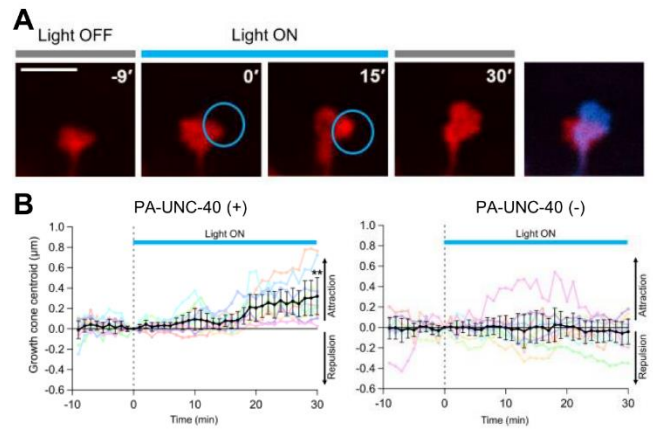


Fig. 6. Light-induced growth cone attraction in *C. elegans*. **A.** Time lapse images showing light-induced VD growth cone attraction. Illuminated regions with blue laser light (2 s min^{-1} pulses, 488 nm) were represented as white circles. Scale bar, 3 μm . **B.** Temporal centroid plots of periodically illuminated growth cones. Each data is represented by a colored line. Averaged data are shown as black. Black bars indicate the illumination periods. Error bars, 98% confidential intervals ($n = 10$). * $P < 0.05$ versus PA-UNC-40 (-) at 30 min, unpaired t -test.

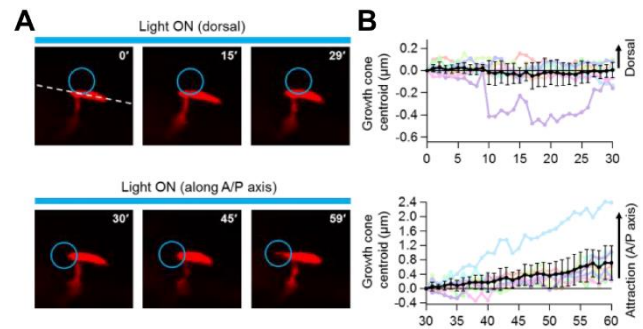


Fig. 7. Photo-manipulation of anvil-shaped growth cones. **A.** Partial illumination of the anvil-shaped growth cone. First, blue light (2 s min^{-1} pulses, 488 nm) was exposed to the dorsal side (0–29 min). Subsequently, the anterior side was illuminated (30–59 min). White dotted line represents the lateral nerve cord. Scale bar, 3 μm . **B.** Temporal centroid plots of the illuminated anvil-shaped growth cones. Second illuminations were performed on either side of the growth cones along the anterior-posterior axis. Each experimental trial is shown with the same colored line. Error bars, 98% confidential intervals ($n = 10$).